

## Relativistic many-body calculations of energy levels, hyperfine constants, and transition rates for sodiumlike ions, $Z=11-16$

M. S. Safronova, A. Derevianko, and W. R. Johnson

*Department of Physics, Notre Dame University, Notre Dame, Indiana 46556*

(Received 12 February 1998)

All-order relativistic many-body calculations of removal energies are carried out for  $3s$ ,  $3p_{1/2}$ ,  $3p_{3/2}$ ,  $3d_{3/2}$ ,  $3d_{5/2}$ , and  $4s$  states of sodium and sodiumlike ions with nuclear charges  $Z$  in the range 12–16. Hyperfine constants are evaluated for each state, and reduced dipole matrix elements are determined for  $3p_{1/2}-3s$ ,  $3p_{3/2}-3s$ ,  $3d_{3/2}-3p_{1/2}$ ,  $3d_{3/2}-3p_{3/2}$ ,  $3d_{5/2}-3p_{3/2}$ ,  $4s-3p_{1/2}$ , and  $4s-3p_{3/2}$  transitions. The calculations include single and double excitations of the Hartree-Fock ground state to all orders in perturbation theory. Corrections to energies are made for a dominant class of triple excitations. The Breit interaction, with all-order correlation corrections, is evaluated. Reduced-mass and mass-polarization corrections are included to third order in perturbation theory. The predicted removal energies, when corrected for the Lamb shift, agree with experiment at the  $1-20\text{-cm}^{-1}$  level of accuracy for all states considered. Theoretical fine-structure intervals agree with measurements to about 0.3% for  $3p$  states and to about 3% for  $3d$  states. Theoretical hyperfine constants and line strengths agree with precise measurements to better than 0.3%. [S1050-2947(98)01308-0]

PACS number(s): 31.25.Jf, 31.15.Dv, 32.10.Fn, 32.70.Cs

### I. INTRODUCTION

In the present paper, we calculate removal energies and hyperfine constants for  $3s$ ,  $3p_{1/2}$ ,  $3p_{3/2}$ ,  $3d_{3/2}$ ,  $3d_{5/2}$ , and  $4s$  states of sodiumlike ions with nuclear charges in the range  $Z=11-16$ . In addition, we calculate reduced dipole matrix elements for  $3p_{1/2}-3s$ ,  $3p_{3/2}-3s$ ,  $4s-3p_{1/2}$ ,  $4s-3p_{3/2}$ ,  $3d_{3/2}-3p_{1/2}$ ,  $3d_{3/2}-3p_{3/2}$ , and  $3d_{5/2}-3p_{3/2}$  electric-dipole transitions. These calculations are based on the relativistic single-double (SD) equations used in Ref. [1] to study Li and  $\text{Be}^+$ , in Ref. [2] to study Li, Na, and Cs, and in Ref. [3] to study Cs. The present calculations complement, and in part supersede, earlier third-order relativistic many-body perturbation theory (MBPT) calculations [4], in which removal energies of  $3s$ ,  $3p_{1/2}$ , and  $3p_{3/2}$  states of sodiumlike ions were evaluated throughout the sodium isoelectronic sequence. For  $Z < 16$ , the differences between the MBPT calculations and measured removal energies ( $\approx 100\text{ cm}^{-1}$ ) are due to omitted correlation corrections, while for higher  $Z$  the differences between theory and experiment were dominated by omitted QED corrections [5].

The ‘‘experimental’’ correlation energy of the  $3s_{1/2}$  state in Na I is found to be about  $1500\text{ cm}^{-1}$  after subtracting the Dirac-Hartree-Fock (DHF) energy, the Breit energy, the reduced-mass correction, and the mass-polarization correction from the experimental ionization energy. The DHF energy is precisely known and the other three corrections are tiny for Na I. The second- and third-order correlation energies are  $1293$  and  $80\text{ cm}^{-1}$ , respectively, from which one infers that  $127\text{ cm}^{-1}$  come from fourth and higher orders. Since the third-order MBPT correlation energy disagrees with the ‘‘experimental’’ correlation energy by 8.5% for the  $3s$  state of Na I, it is clearly of interest to carry out all-order

calculations.<sup>1</sup> It is also of interest to determine the point in the sodium isoelectronic sequence beyond which all-order calculations are no longer necessary and third-order MBPT gives 99% or more of the correlation energy. In this paper, we use the all-order SD approximation to study these questions in low- $Z$  sodiumlike ions.

To evaluate the higher-order correlation corrections, we solve the relativistic SD equations, which are linearized coupled-cluster single-double (CCSD) equations [6] that include single and double excitations of the DHF wave function to all orders in perturbation theory. In our calculations, corrections are also made for a dominant class of triple excitations. The resulting energies and matrix elements are complete through third order in perturbation theory, and include important contributions from fourth and higher orders. The Breit interaction, which is very sensitive to correlation, is included by calculating the matrix element of the two-body Breit operator using SD wave functions; it, therefore, includes Coulomb correlation corrections to all orders in perturbation theory. Mass-polarization corrections are treated to third order in perturbation theory following the procedure described in Ref. [4].

We also use the SD wave functions to evaluate hyperfine constants for the states considered, and  $E1$  reduced matrix elements for transitions between these states. The present

<sup>1</sup>The third-order correlation energy for sodium given above differs from the value given in Ref. [4], which was obtained by summing partial waves  $l=0-4$  and omitting contributions from the  $1s^2$  core shell. To obtain more accurate values, we recalculated the third-order energies along the isoelectronic sequence including all shells, summed partial waves  $l=0-6$ , and extrapolated the partial-wave sequence to obtain the  $l \geq 7$  remainder.

calculations supersede previous third-order MBPT calculations of hyperfine constants for sodium [7], which were accurate to about 3%, and third-order calculations of  $3p$ - $3s$  and  $4s$ - $3p$  transition rates [8], which differ from recent measurements in sodium [9] by about 1%.

For neutral sodium, previous SD calculations [2,10], CCSD calculations [11], and configuration-interaction calculations [12], all give values for hyperfine constants and transition rates that agree with experiment to within a fraction of a percent. The previous SD and the CCSD calculations also give removal energies in close agreement with experiment.

The present SD calculations give removal energies for Na I accurate to better than  $2 \text{ cm}^{-1}$ , and give hyperfine constants and dipole line strengths that agree with precise experiments to better than 0.3%. The SD method also gives removal energies for sodiumlike ions,  $Z=12$ – $16$ , that agree with experiment at the level  $1$ – $20 \text{ cm}^{-1}$  assuming that Lamb-shift corrections are made for  $3s$  states. From the comparison of the present all-order correlation energies with previous third-order calculations, we find that fourth- and higher-order corrections are less than 1% of the correlation energy for  $Z>20$ . The present calculations bridge the gap from Na I, where correlation corrections are much larger than relativistic corrections, to S VI, where higher-order correlation corrections are much smaller than relativistic corrections.

## II. METHOD

The relativistic SD equations were discussed at length in Refs. [1–3], so we will give only a brief reprise of the equations here. In the SD approach, the wave function  $\Psi_v$  of an atomic system with one valence electron is represented as

$$\Psi_v = \left[ 1 + \sum_{ma} \rho_{ma} a_m^\dagger a_a + \frac{1}{2} \sum_{mnab} \rho_{mnab} a_m^\dagger a_n^\dagger a_b a_a + \sum_{m \neq v} \rho_{mv} a_m^\dagger a_v + \sum_{mna} \rho_{mnva} a_m^\dagger a_n^\dagger a_a a_v \right] \Phi_v, \quad (1)$$

where  $\Phi_v$  is the lowest-order atomic state function, which is taken to be the *frozen-core* Dirac-Hartree-Fock wave function of a state  $v$ . In this equation,  $a_i^\dagger$  and  $a_i$  are creation and annihilation operators, respectively, for state  $i$ . Here and below, we use the convention that indices at the beginning of the alphabet ( $a, b, \dots$ ), refer to occupied core states, those in the middle of the alphabet ( $m, n, \dots$ ), refer to excited states, and  $v$  and  $w$  refer to valence orbitals. We use indices  $i, j, k$ , and  $l$  to describe arbitrary orbitals.

The coefficients  $\rho_{ma}$  and  $\rho_{mnab}$  are amplitudes for single and double excitations from the core, respectively;  $\rho_{mv}$  is the amplitude for a single excitation of the valence electron, and  $\rho_{mnva}$  is the amplitude for excitation of the valence electron and a core electron. Substituting the wave function (1) into the many-body Schrödinger equation, where the Hamiltonian is taken to be the relativistic *no-pair* Hamiltonian [13] with Coulomb interactions, one obtains the coupled equations for single- and double-excitation coefficients written down in Sec. II A.

### A. Coupled equations for singles and doubles

The coupled equations for the core excitation coefficients are [1]

$$(\epsilon_a - \epsilon_m) \rho_{ma} = \sum_{bn} \tilde{g}_{mban} \rho_{nb} + \sum_{bnr} g_{mbnr} \tilde{\rho}_{nrab} - \sum_{bcn} g_{bcan} \tilde{\rho}_{mnbc}, \quad (2)$$

$$\begin{aligned} (\epsilon_a + \epsilon_b - \epsilon_m - \epsilon_n) \rho_{mnab} &= g_{mnab} + \sum_{cd} g_{cdab} \rho_{mncd} + \sum_{rs} g_{mnr s} \rho_{rsab} \\ &+ \left[ \sum_r g_{mnr b} \rho_{ra} - \sum_c g_{cnab} \rho_{mc} + \sum_{rc} \tilde{g}_{cnrb} \tilde{\rho}_{mrac} \right] \\ &+ \left[ \begin{array}{l} a \leftrightarrow b \\ m \leftrightarrow n \end{array} \right]. \end{aligned} \quad (3)$$

Here  $\epsilon_i$  is the single-body DHF energy for the state  $i$ . The quantities  $g_{ijkl}$  are two-body Coulomb matrix elements, and  $\tilde{g}_{ijkl} = g_{ijkl} - g_{ijlk}$  are antisymmetrized Coulomb matrix elements. Antisymmetrized excitation amplitudes are designated by  $\tilde{\rho}_{ijkl} = \rho_{ijkl} - \rho_{ijlk}$ . The correlation correction to the core energy is given in terms of the core excitation amplitudes by

$$\delta E_c = \frac{1}{2} \sum_{mnab} g_{abmn} \tilde{\rho}_{mnab}. \quad (4)$$

The equations governing the valence excitation amplitudes are

$$\begin{aligned} (\epsilon_v - \epsilon_m + \delta E_v) \rho_{mv} &= \sum_{bn} \tilde{g}_{mbvn} \rho_{nb} + \sum_{bnr} g_{mbnr} \tilde{\rho}_{nr vb} \\ &- \sum_{bcn} g_{bcvn} \tilde{\rho}_{mnbc}, \end{aligned} \quad (5)$$

$$\begin{aligned} (\epsilon_v + \epsilon_b - \epsilon_m - \epsilon_n + \delta E_v) \rho_{mnvb} &= g_{mnvb} + \sum_{cd} g_{cdvb} \rho_{mncd} + \sum_{rs} g_{mnr s} \rho_{rsvb} \\ &+ \left[ \sum_r g_{mnr b} \rho_{rv} - \sum_c g_{cnvb} \rho_{mc} + \sum_{rc} \tilde{g}_{cnrb} \tilde{\rho}_{mrvc} \right] \\ &+ \left[ \begin{array}{l} v \leftrightarrow b \\ m \leftrightarrow n \end{array} \right], \end{aligned} \quad (6)$$

where  $\delta E_v$  is the correlation correction to the valence energy for the state  $v$ , which is given in terms of the excitation amplitudes by

$$\delta E_v = \sum_{ma} \tilde{g}_{vavm} \rho_{ma} + \sum_{mab} g_{abvm} \tilde{\rho}_{mvab} + \sum_{mna} g_{vbmn} \tilde{\rho}_{mnvb}. \quad (7)$$

To solve Eqs. (2)–(7), an angular momentum decomposition is first carried out, and the equations are then reduced to coupled equations involving single-body radial wave functions only. The radial wave functions for states  $v, m, n, a, b, \dots$  are taken from a  $B$ -spline basis set [14], and the resulting coupled radial equations are solved iteratively. The core equations (2) and (3) are solved first, and the valence equations (5)–(7) are then solved successively for each of the six states being considered using the converged core amplitudes.

### B. Triple excitations and perturbation theory

One can show that the core correlation energy  $\delta E_c$  obtained from Eq. (4) is complete through third order in perturbation theory. The valence correlation energy  $\delta E_v$  given in Eq. (7), by contrast, includes only part of the third-order correlation energy. Indeed, the third-order contribution to the energy obtained by iterating Eqs. (2) and (3) and (5) and (6) once, substituting into Eq. (7), and omitting second- and fourth-order terms, is

$$\begin{aligned} \delta E_v^{(3)} = & \sum_{mabcd} \frac{\tilde{g}_{abvm} \tilde{g}_{cdab} \tilde{g}_{mvcd}}{(\epsilon_{ab} - \epsilon_{vm})(\epsilon_{cd} - \epsilon_{mv})} + \sum_{mabrs} \frac{\tilde{g}_{abvm} \tilde{g}_{mvr} \tilde{g}_{rsab}}{(\epsilon_{ab} - \epsilon_{vm})(\epsilon_{ab} - \epsilon_{rs})} + \sum_{mabcr} \frac{\tilde{g}_{abvm} \tilde{g}_{cvrb} \tilde{g}_{mrac}}{(\epsilon_{ab} - \epsilon_{vm})(\epsilon_{ac} - \epsilon_{mr})} \\ & + \sum_{mabcr} \frac{\tilde{g}_{abvm} \tilde{g}_{cmra} \tilde{g}_{vrbc}}{(\epsilon_{ab} - \epsilon_{vm})(\epsilon_{bc} - \epsilon_{vr})} + \sum_{mabnr} \frac{\tilde{g}_{vavm} \tilde{g}_{mbnr} \tilde{g}_{nrab}}{(\epsilon_a - \epsilon_m)(\epsilon_{ab} - \epsilon_{nr})} - \sum_{mabcn} \frac{\tilde{g}_{vavm} \tilde{g}_{bcna} \tilde{g}_{mnbc}}{(\epsilon_a - \epsilon_m)(\epsilon_{bc} - \epsilon_{mn})} \\ & + \sum_{mnbcd} \frac{\tilde{g}_{vbm} \tilde{g}_{cdvb} \tilde{g}_{mncd}}{(\epsilon_{vb} - \epsilon_{mn})(\epsilon_{cd} - \epsilon_{mn})} + \sum_{mnbrc} \frac{\tilde{g}_{vbm} \tilde{g}_{mnr} \tilde{g}_{rsvb}}{(\epsilon_{vb} - \epsilon_{mn})(\epsilon_{vb} - \epsilon_{rs})} + \sum_{mnbrc} \frac{\tilde{g}_{vbm} \tilde{g}_{cnrb} \tilde{g}_{mrvc}}{(\epsilon_{vb} - \epsilon_{mn})(\epsilon_{vc} - \epsilon_{mr})} \\ & + \sum_{mnbrc} \frac{\tilde{g}_{vbm} \tilde{g}_{cmrv} \tilde{g}_{nrbc}}{(\epsilon_{vb} - \epsilon_{mn})(\epsilon_{bc} - \epsilon_{nr})}, \end{aligned} \quad (8)$$

which differs from the results of third-order MBPT given in Ref. [15]. The missing third-order terms are accounted for entirely by adding triple excitations of the form

$$\frac{1}{6} \sum_{abmnr} \rho_{mnr} a_m^\dagger a_n^\dagger a_r^\dagger a_v a_b a_a \Phi_v$$

to the right-hand side of the wave function in Eq. (1). The contribution of this term to the valence energy is

$$E_{v \text{ extra}} = \frac{1}{2} \sum_{mnab} \tilde{g}_{abmn} \rho_{mnr} \quad (9)$$

When this term is evaluated to lowest nonvanishing order (third order), it leads to the following contribution to the correlation energy:

$$\begin{aligned} E_{v \text{ extra}}^{(3)} = & \sum_{mnabc} \frac{\tilde{g}_{abmn} \tilde{g}_{cmav} \tilde{g}_{nvbc}}{(\epsilon_{ab} - \epsilon_{mn})(\epsilon_{bc} - \epsilon_{nv})} + \sum_{mnabs} \frac{\tilde{g}_{abmn} \tilde{g}_{nvas} \tilde{g}_{msvb}}{(\epsilon_{ab} - \epsilon_{mn})(\epsilon_{vb} - \epsilon_{ms})} + \sum_{mnabc} \frac{\tilde{g}_{abmn} \tilde{g}_{cvbv} \tilde{g}_{mnca}}{(\epsilon_{ab} - \epsilon_{mn})(\epsilon_{ca} - \epsilon_{mn})} \\ & + \sum_{mnabs} \frac{\tilde{g}_{abmn} \tilde{g}_{mvsv} \tilde{g}_{nsba}}{(\epsilon_{ab} - \epsilon_{mn})(\epsilon_{ab} - \epsilon_{ns})} + \sum_{mnabs} \frac{\tilde{g}_{abmn} \tilde{g}_{mnvs} \tilde{g}_{vsba}}{(\epsilon_{ab} - \epsilon_{mn})(\epsilon_{ab} - \epsilon_{vs})} + \sum_{mnabc} \frac{\tilde{g}_{abmn} \tilde{g}_{cvba} \tilde{g}_{mnvc}}{(\epsilon_{ab} - \epsilon_{mn})(\epsilon_{vc} - \epsilon_{mn})} \\ & + \sum_{mnabc} \frac{\tilde{g}_{abmn} \tilde{g}_{cmab} \tilde{g}_{vnvc}}{(\epsilon_{ab} - \epsilon_{mn})(\epsilon_c - \epsilon_n)} + \sum_{mnabs} \frac{\tilde{g}_{abmn} \tilde{g}_{mnas} \tilde{g}_{vsvb}}{(\epsilon_{ab} - \epsilon_{mn})(\epsilon_b - \epsilon_s)}. \end{aligned} \quad (10)$$

The sum  $\delta E_v^{(3)} + E_{v \text{ extra}}^{(3)}$  gives the entire third-order valence correlation energy [15]. In our final tabulations, we add  $E_{v \text{ extra}}^{(3)}$  to the SD correlation energy  $\delta E_v$  to account for the missing third-order terms.

### C. Matrix elements of one-body operators

The formalism for calculating matrix elements of a one-body operator  $Z$  in the SD approach was developed in Ref.

[1], where it was applied to determine hyperfine constants and transition matrix elements for Li and Be<sup>+</sup>. Here, we apply the formalism to calculations of electric-dipole matrix elements, as well as  $A$  and  $B$  hyperfine constants along the sodium isoelectronic sequence. A one-body operator is represented in second quantization as

$$Z = \sum_{ij} z_{ij} a_i^\dagger a_j, \quad (11)$$

where  $z_{ij}$  is the matrix element of the operator  $z$  between single-particle orbitals. Here,  $z$  is the coordinate operator when one is evaluating dipole transition matrix elements or the hyperfine operator written down and discussed in Ref. [16] when one is evaluating the magnetic-dipole hyperfine constant. Substituting wave functions of the form Eq. (1) into the matrix element  $\langle \Psi_w | Z | \Psi_v \rangle$ , and correcting for normalization, one obtains the size-consistent expression [1]

$$\langle \Psi_w | Z | \Psi_v \rangle = \delta_{wv} Z_{\text{core}} + \frac{Z_{\text{val}}}{[(1 + \delta N_w)(1 + \delta N_v)]^{1/2}}. \quad (12)$$

The term  $Z_{\text{val}}$  consists of the lowest-order (DHF) matrix element  $z_{wv}$  corrected by a set of 20 terms, given together with normalization correction  $\delta N_v$  in Ref. [1]. Two of the important contributions to  $Z_{\text{val}}$  are the random-phase-approximation (RPA)-like term  $Z_{wv}^{\text{RPA}}$ , and the polarization-like [Brueckner orbital (BO)] correction  $Z_{wv}^{\text{BO}}$ , given by

$$Z_{wv}^{\text{RPA}} = \sum_{am} z_{am} \tilde{\rho}_{wmva} + \text{c.c.},$$

$$Z_{wv}^{\text{BO}} = \sum_m z_{wm} \rho_{mv} + \text{c.c.}$$

The remaining 18 contributions to  $Z_{\text{val}}$  are linear or quadratic functions of the SD excitation amplitudes that can be evaluated once the SD equations are solved. The term  $Z_{\text{core}}$  contributes only for scalar operators; it was written down and discussed recently in Ref. [17].

#### D. Expectation value of the Breit operator

The atomic Hamiltonian employed to determine the wave functions did not contain the Breit interaction. The contribution of the Breit interaction to the removal energies is found by calculating the expectation value of Breit operator  $\hat{B}$ :

$$B_v^{\text{SD}} = \langle \Psi_v | \hat{B} | \Psi_v \rangle.$$

This expression treats the Breit interaction to first order, but includes Coulomb corrections to all orders. In Ref. [4], the Breit energy shift was evaluated to third order in MBPT (first-order Breit and second-order Coulomb) including RPA and polarization corrections. A strong dependence of the Breit interaction on correlation effects was found in these MBPT calculations. To study this problem further, we calculate the expectation value of the Breit operator using the SD wave function  $\Psi_v$ . The SD approach is expected to be more accurate, since the SD approximation recovers the entire third-order contribution for one-body operators, and contains polarization corrections and the dominant RPA corrections as a subclass of all-order diagrams.

The two-body Breit operator can be represented in the static limit as

$$\hat{B} = \frac{1}{2} \sum_{ijkl} b_{ijkl} a_i^\dagger a_j^\dagger a_l a_k, \quad (13)$$

where

$$b_{ijkl} = -\langle ij | \frac{\alpha_1 \cdot \alpha_2 + (\alpha_1 \cdot \hat{r}_{12})(\alpha_2 \cdot \hat{r}_{12})}{2r_{12}} | kl \rangle. \quad (14)$$

Let us outline the formalism used to determine matrix elements of two-body operators. Any two-body operator  $B$  can be decomposed as a sum of normally ordered zero-body  $B^{(0)}$ , one-body  $B^{(1)}$ , and two-body  $B^{(2)}$  operators:

$$B^{(0)} = \frac{1}{2} \sum_{ab} \tilde{b}_{abab}, \quad (15)$$

$$B^{(1)} = \sum_{ij} \left( \sum_a \tilde{b}_{iaja} \right) : a_i^\dagger a_j :, \quad (16)$$

$$B^{(2)} = \frac{1}{2} \sum_{ijkl} b_{ijkl} : a_i^\dagger a_j^\dagger a_l a_k :. \quad (17)$$

Here  $::$  denotes the normal form of operator products. The zero-body operator  $B^{(0)}$  does not contribute to valence removal energies. The calculation of the matrix element of the one-body operator  $B^{(1)}$  follows exactly the pattern described previously for the operator  $Z$ . The matrix element of the two-body operator  $B^{(2)}$  is more complicated, leading to 36 distinct terms. These terms can be classified by an ‘‘effective’’ MBPT order, taking into account that single excitations  $\rho_{ij}$  appear in the expression for the wave function starting in second order of MBPT, while double excitations  $\rho_{ijkl}$  appear starting in first order. We assume that the major contribution to  $B^{(2)}$  arises from the second effective order. There are two such terms contributing to the valence removal energies

$$B_a^{(2)} = \sum_{amn} b_{mnva} \tilde{\rho}_{mnva} + \text{c.c.}, \quad (18)$$

$$B_b^{(2)} = \sum_{abm} b_{mvab} \tilde{\rho}_{vmab} + \text{c.c.} \quad (19)$$

The expression for the normalized two-body matrix element in second effective order is similar to the corresponding expression (12) for the one-body operator  $Z$ :

$$B_{\text{norm}}^{(2)} = \frac{B_a^{(2)} + B_b^{(2)}}{1 + \delta N_v}. \quad (20)$$

TABLE I. Partial-wave contributions to  $\delta E_v$  ( $\text{cm}^{-1}$ ) for Al III. The row labeled Err. contains an estimate of the extrapolation error.

$l$	$3s$	$3p_{1/2}$	$3p_{3/2}$	$4s$	$3d_{3/2}$	$3d_{5/2}$
0	56.1	94.4	94.0	10.7	-0.7	-0.7
1	-506.8	-168.9	-166.4	-164.8	-88.0	-88.4
2	-2688.9	-1785.8	-1774.6	-749.0	-465.5	-465.0
3	-2990.3	-2014.9	-2002.4	-829.0	-1001.1	-1004.4
4	-3057.6	-2080.4	-2067.6	-847.1	-1080.8	-1080.1
5	-3080.9	-2100.4	-2087.5	-853.5	-1103.8	-1103.0
6	-3090.9	-2108.5	-2095.6	-856.3	-1110.8	-1110.0
$\delta E_v$	-3106.1	-2120.4	-2107.5	-860.6	-1115.1	-1114.3
Err.	1.9	1.0	0.9	0.5	5.9	6.0

TABLE II. Contributions to the removal energies ( $\text{cm}^{-1}$ ) for sodiumlike ions,  $Z=11-16$ .

Term	$3s$	$3p_{1/2}$	$3p_{3/2}$	$4s$	$3d_{3/2}$	$3d_{5/2}$
Na I						
$E_v^{\text{DHF}}$	-39951.6	-24030.4	-24014.1	-15398.9	-12217.4	-12217.5
$\delta E_v$	-1488.8	-463.9	-461.6	-308.5	-58.9	-58.9
$E_v^{(3)\text{extra}}$	-9.2	-1.5	-1.6	-2.1	1.0	1.0
$B_v^{\text{SD}}$	1.2	1.4	0.1	0.3	-0.1	-0.1
RM+MP	1.0	0.5	0.5	0.4	0.3	0.3
$E_{\text{tot}}$	-41447.3	-24493.9	-24476.7	-15708.7	-12275.1	-12275.1
$E_{\text{expt}}$	-41449.4	-24493.3	-24476.1	-15709.4	-12276.6	-12276.6
Err.	0.4	0.0	0.0	0.1	0.0	0.0
Mg II						
$E_v^{\text{DHF}}$	-118824.0	-84293.9	-84203.6	-50858.1	-49341.2	-49342.0
$\delta E_v$	-2462.2	-1322.3	-1315.0	-609.9	-433.5	-433.4
$E_v^{(3)\text{extra}}$	12.0	4.7	4.6	4.6	4.3	4.3
$B_v^{\text{SD}}$	6.9	8.9	2.7	2.0	-0.4	-0.6
RM+MP	2.8	1.5	1.5	1.2	1.0	1.0
$E_{\text{tot}}$	-121264.6	-85601.1	-85509.8	-51460.2	-49769.8	-49770.7
$E_{\text{expt}}$	-121267.6	-85598.3	-85506.8	-51462.7	-49776.6	-49777.4
Err.	1.0	0.3	0.3	0.2	1.4	1.4
Al III						
$E_v^{\text{DHF}}$	-226396.4	-173686.9	-173452.1	-102439.3	-112371.9	-112373.9
$\delta E_v$	-3106.1	-2120.4	-2107.5	-860.6	-1115.1	-1114.3
$E_v^{(3)\text{extra}}$	33.5	18.4	18.2	12.5	10.2	10.1
$B_v^{\text{SD}}$	17.3	23.8	9.3	5.3	-0.8	-1.8
RM+MP	4.6	2.5	2.5	2.2	1.7	1.7
$E_{\text{tot}}$	-229447.0	-175762.6	-175529.6	-103280.0	-113475.9	-113478.2
$E_{\text{expt}}$	-229445.7	-175762.8	-175529.1	-103281.6	-113487.2	-113489.5
Err.	1.9	1.0	0.9	0.5	5.9	6.0
Si IV						
$E_v^{\text{DHF}}$	-360613.7	-290073.8	-289606.1	-169076.7	-201807.3	-201807.4
$\delta E_v$	-3578.3	-2809.3	-2790.6	-1071.8	-1915.8	-1913.1
$E_v^{(3)\text{extra}}$	49.4	32.3	31.9	19.0	18.9	18.7
$B_v^{\text{SD}}$	33.1	47.3	21.1	10.6	0.1	-3.5
RM+MP	6.9	3.7	3.7	3.4	2.4	2.4
$E_{\text{tot}}$	-364102.5	-292799.8	-292340.0	-170115.6	-203701.8	-203702.8
$E_{\text{expt}}$	-364093.1	-292805.6	-292344.5	-170114.2	-203717.5	-203718.7
Err.	2.2	1.4	1.6	0.8	13.0	13.0
P V						
$E_v^{\text{DHF}}$	-520666.6	-432533.4	-431722.3	-250303.9	-317578.4	-317567.4
$\delta E_v$	-3945.9	-3397.9	-3372.7	-1252.1	-2700.6	-2694.9
$E_v^{(3)\text{extra}}$	60.3	43.9	43.4	24.0	28.7	28.5
$B_v^{\text{SD}}$	55.1	80.8	39.1	18.2	3.5	-4.9
RM+MP	9.0	4.8	4.8	4.5	2.9	2.9
$E_{\text{tot}}$	-524488.1	-435801.7	-435007.7	-251509.4	-320243.8	-320235.7
$E_{\text{expt}}$	-524462.9	-435811.0	-435015.6	-251503.6	-320263.9	-320256.9
Err.	3.3	2.8	2.6	1.0	21.3	21.3
S VI						
$E_v^{\text{DHF}}$	-706161.1	-600593.4	-599302.4	-345878.2	-459392.4	-459354.6
$\delta E_v$	-4242.8	-3901.8	-3870.1	-1407.9	-3412.6	-3402.9
$E_v^{(3)\text{extra}}$	67.6	53.0	52.3	28.2	38.3	38.0
$B_v^{\text{SD}}$	84.1	125.9	64.2	28.4	10.7	-5.4
RM+MP	11.7	6.2	6.2	6.0	3.6	3.6
$E_{\text{tot}}$	-710240.5	-604310.2	-603049.8	-347223.5	-462752.5	-462721.3
$E_{\text{expt}}$	-710194.7	-604321.1	-603057.0	-347205.9	-462772.2	-462739.7
Err.	4.6	4.2	4.3	1.6	29.9	29.8

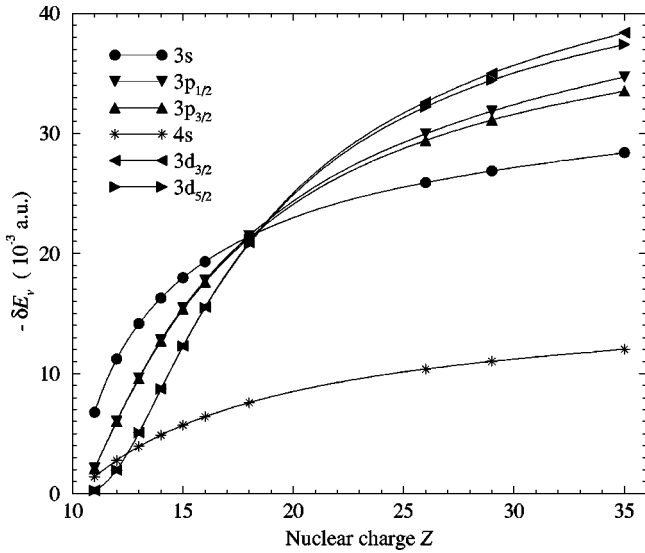


FIG. 1. The SD correlation corrections  $\delta E_v$  to valence removal energies as functions of  $Z$  for sodiumlike ions.

For a more detailed description, the reader is referred to Ref. [17], where the “effective”-order formalism was applied to the calculation of the static atom-wall interaction constant  $C_3$ .

### III. VALENCE REMOVAL ENERGIES

The SD correlation energies  $\delta E_v$  for  $3s$ ,  $3p_{1/2}$ ,  $3p_{3/2}$ ,  $3d_{3/2}$ ,  $3d_{5/2}$ , and  $4s$  states of sodium and sodiumlike ions with nuclear charges  $Z=12-16$  are found from Eq. (7). As mentioned previously, we first solve the core equations (2) and (3) completely, and then solve the valence equations (5)–(7) successively for each of the six states being considered. We retain terms in the angular-momentum decomposition from single-body states with  $l=0-6$ , and extrapolate to obtain the final correlation energies. We limit our basis set to  $n=27$  out of 30 spline basis functions for each value of  $l$ . The convergence pattern of the partial-wave sequence and our estimate of the numerical uncertainty is illustrated in Table I for the case of Al III. The procedures used to extrapolate  $\delta E_v$  and estimate extrapolation errors (listed as Err. in Tables I and II) are described in the Appendix.

In Fig. 1, we plot the all-order correlation energy  $\delta E_v$  against nuclear charge  $Z$  for the six states considered. Contributions for  $Z=18, 26, 29$ , and  $35$  are also included here and in the next three figures to help clarify the  $Z$  dependence. The graphs in Fig. 1 are dominated by the second-order correlation energy, which is 80–90% of  $\delta E_v$  over the range considered. For neutral sodium, the correlation energy is seen to be largest for the  $3s$  state; however, at higher  $Z$  the correlation energy is largest for the  $3d$  states. For neutral sodium, the  $3d_{3/2}$  and  $3d_{5/2}$  correlation energies are small (about  $60 \text{ cm}^{-1}$ ), but they increase very rapidly with  $Z$ . Since the second-order energy determines the shapes of the curves in Fig. 1, we plot  $\delta E_v - E_v^{(2)}$  in Fig. 2 to gain a more detailed view of third- and higher-order contributions given by the SD method. This graph shows that these contributions still grow very rapidly at  $Z=16$ ; a somewhat unexpected result. In Fig. 3, contributions to the correlation energy from

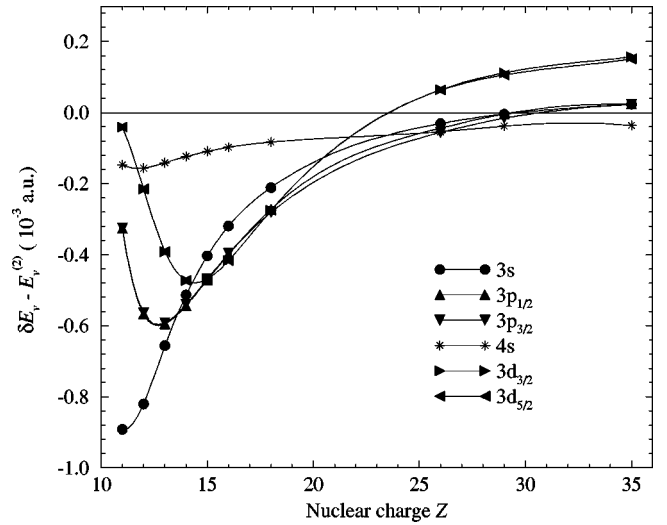


FIG. 2. Third- and higher-order corrections  $\delta E_v - E_v^{(2)}$  to valence removal energies as functions of  $Z$  for sodiumlike ions.

$E_v^{(3)}$  are plotted. These contributions are small for sodium, but grow very rapidly with  $Z$ . For the highest  $Z$  considered ( $Z=35$ ),  $E_v^{(3)}$  is 85% of  $E_v^{(2)}$  for the  $3s$  state and of comparable size for the other states considered. In Fig. 4, we show  $E_v^{\text{corr}} - E_v^{(2+3)}$ , where  $E_v^{\text{corr}} = \delta E_v + E_v^{(3)}$ . These are the contributions to the correlation energy of fourth and higher orders. (In preparing this figure, only the second-order energies were extrapolated to avoid introducing additional extrapolation errors into the small differences shown.) The higher-order correlation contributions are seen to decrease by a factor of 6 over the range  $Z=11-35$  for  $3s$  states. For  $4s$ ,  $3p$ , and  $3d$  states the higher-order corrections have maxima at  $Z=12, 13$ , and  $15$ , respectively. The relative size of the higher-order correlation corrections decreases from 6–9% for  $Z=11$  to 1% for  $Z=20$ . For  $Z>20$ , third-order MBPT, therefore, recovers more than 99% of the correlation energy.

In Table II, we list the various contribution to the removal energies of  $3s$ ,  $3p_{1/2}$ ,  $3p_{3/2}$ ,  $4s$ ,  $3d_{3/2}$ , and  $3d_{5/2}$  states of ions with  $Z=11-16$ . The zeroth-order DHF energy is given

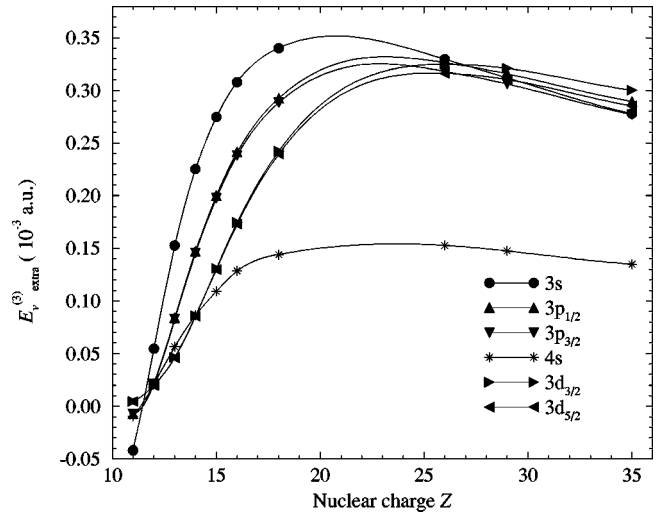


FIG. 3. Contributions to the valence removal energies from  $E_v^{(3)}$  as functions of  $Z$  for sodiumlike ions.

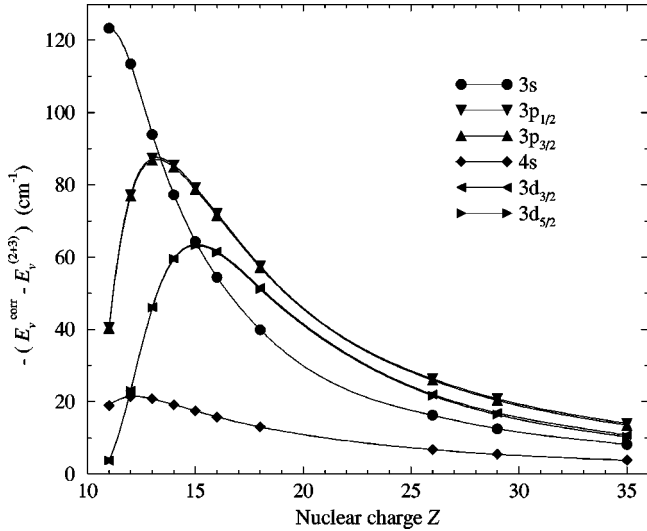


FIG. 4. Fourth- and higher-order correlation corrections to the valence removal energies as functions of  $Z$  for sodiumlike ions.

in the row labeled  $E_v^{\text{DHF}}$ . The row labeled  $\delta E_v$  lists all-order results obtained by calculating the first seven partial waves, and extrapolating the remainder as explained in the Appendix. The row labeled  $E_v^{\text{extra}(3)}$  is the “extra” third-order contribution given in Eq. (10). The relative contribution of  $E_v^{\text{extra}(3)}$  increases with  $Z$  to about 1.6% of the correlation energy for the  $3s$  state in S VI and its absolute value for this state is large,  $68 \text{ cm}^{-1}$ . Clearly, this contribution cannot be omitted in precision calculations. The row labeled  $B_v^{\text{SD}}$  gives the Breit contribution evaluated as the expectation value of the Breit operator using SD wave functions. The evaluation of the Breit correction is discussed further in Sec. IV C. The row labeled RM+MP contains the sum of the reduced-mass and mass-polarization corrections, which are evaluated to third order using the method described in Ref. [4]. The row labeled  $E_{\text{tot}}$  lists the theoretical energy, which is the sum of all of the above contributions. The row labeled  $E_{\text{expt}}$  gives experimental removal energies taken from the National Institute of Standards and Technology database [18]. Finally, the row labeled Err. gives our estimate of the numerical uncertainty in the theoretical energies. Note that this uncertainty grows with  $Z$  because the correlation energy increases with  $Z$ . The relatively large value of Err. for  $3d$  states is a result of the fact that including only seven partial waves permits us to extrapolate the  $3d$  correlation energies with only 1% accuracy for  $Z > 13$ .

Differences between the theoretical and experiment energies for  $3s$  states of ions with  $Z \leq 13$  range from 1 to  $3 \text{ cm}^{-1}$ , but these differences increase rapidly for  $Z > 13$  as shown in Fig. 5. We attribute the major part of the differences for  $Z > 13$  to omitted QED corrections, which are dominated by the  $3s$  self-energy. Codes to evaluate the self-energy in a realistic atomic potential, such as the one described in Ref. [5], do not converge for the low values of  $Z$  considered here, so it is necessary to turn to approximate schemes to estimate QED corrections. In Fig. 5, we show several different estimates. First, we show values of the self-energy obtained by replacing  $Z$  by  $Z-5$ ,  $Z-6$ , and  $Z-7$  in the precisely calculated Coulomb-field self-energies given for  $3s$  states by Mohr and Kim [19]. Next, we compare with values of the

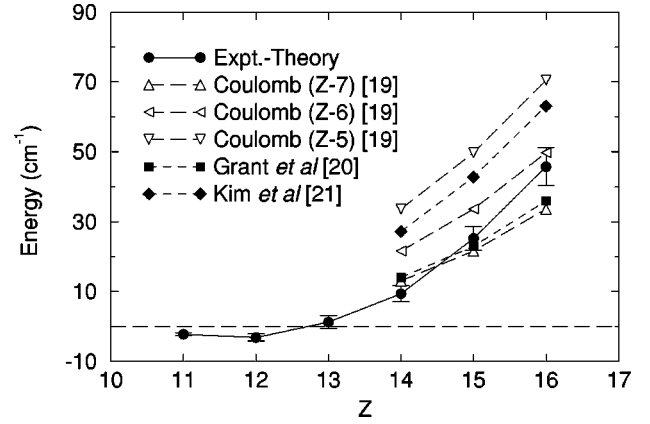


FIG. 5. Differences between experimental and theoretical energies for  $3s$  states of sodiumlike ions are compared with theoretical estimates of the  $3s$  Lamb shift.

Lamb shift from the MCDF code of Grant *et al.* [20], which were also obtained by scaling Coulomb-field values of the self-energy, but contain estimates of vacuum-polarization corrections. Finally, we present values of the Lamb shift from Kim *et al.* [21], determined using Welton’s approximation [22] to the self-energy, and including corrections for vacuum polarization. The values from Ref. [20] agree well with the  $Z-7$  Coulomb values from Ref. [19], while those from Ref. [21] lie between the  $Z-5$  and  $Z-6$  Coulomb-field values. It can be seen that if we add any of these estimates of the Lamb shift to the theoretical energy, the resulting value will be within  $20 \text{ cm}^{-1}$  of the experimental energy. In the absence of more reliable values for the low-order QED corrections, it is impossible to reduce the difference between theory and experiment for these states further.

All-order methods were used previously in Ref. [2] to calculate correlation energies for  $3s$ ,  $3p_{1/2}$ ,  $3p_{3/2}$ , and  $4s$  states of Na I, and in Ref. [11] to calculate correlation energies for the  $3s$  state of Na I. In Table III, we compare our results with these two calculations and with the “experimental” correlation energy. To obtain the experimental correlation energy, we subtracted the DHF energy, the Breit energy, and the reduced mass plus mass polarization corrections from the experimental data [18]. Our value of  $\delta E_v$  is more precise than the SD result from Ref. [2] since, in that work, only partial waves with  $l \leq 4$  were included,  $E_v^{\text{extra}(3)}$  was omitted, and no extrapolation was made. In Ref. [11], accurate nonrelativistic calculations of  $3s$  correlation energy were made using the CCSD approach. Relativistic corrections and certain three-body cluster contributions to the  $3s$  energy were also included in the correlation energy. Although the two calculations account for different classes of

TABLE III. Comparison of the present SD calculations of the correlation energy (a.u.) for Na I with the SD calculations of Ref. [2], the CCSD calculations of Ref. [11], and experiment [18].

State	Present	SD [2]	CCSD [11]	Expt.
$3s$	-0.006835	-0.00657	-0.006840	-0.006825
$3p_{1/2}$	-0.002118	-0.00204		-0.002121
$3p_{3/2}$	-0.002108	-0.00203		-0.002110
$4s$	-0.001418	-0.00136		-0.001415

TABLE IV. Comparison of theoretical and experimental fine-structure intervals ( $\text{cm}^{-1}$ ) for  $3p$  and  $3d$  states in sodium and sodiumlike ions,  $Z=12-16$ . The experimental values are from Ref. [18].

Z	$3p_{3/2}-3p_{1/2}$		$3d_{5/2}-3d_{3/2}$	
	Theory	Expt.	Theory	Expt.
11	17.15	17.20	-0.04	-0.05
12	91.33	91.57	-0.90	-0.87
13	233.13	233.67	-2.32	-2.29
14	459.93	461.10	-1.06	-1.19
15	793.96	795.38	8.10	7.05
16	1260.53	1264.10	31.22	32.50

correlation diagrams, both the present calculation and the CCSD calculation are in close agreement with each other; moreover, they are both in excellent agreement with experiment. We also compared our results for  $3s$ ,  $3p$ , and  $4s$  energies for  $Z=11-14$ , and 16 with multiconfiguration Hartree-Fock (MCHF) calculations [23]. Differences between the nonrelativistic MCHF calculations and the present values of the  $3s$  removal energies ranged from  $54 \text{ cm}^{-1}$  for  $Z=11$  to  $1717 \text{ cm}^{-1}$  for  $Z=16$ . Moreover, the estimates of relativistic shifts given in Ref. [23], which range from  $48 \text{ cm}^{-1}$  for  $Z=11$  to  $1850 \text{ cm}^{-1}$  for  $Z=16$ , do not completely account for observed differences.

In Table IV, we present the  $3p_{3/2}-3p_{1/2}$  and  $3d_{5/2}-3d_{3/2}$  fine-structure intervals. These values were calculated extrapolating the second-order energy only to avoid introducing extrapolation errors into the intervals. Our uncertainties for the  $3p$  intervals range from  $0.2 \text{ cm}^{-1}$  for  $Z=11$  to  $0.4 \text{ cm}^{-1}$  for  $Z=16$ ; the corresponding uncertainties for the  $3d$  splittings are  $0.1-0.2 \text{ cm}^{-1}$ . The third- and higher-order contributions to the splitting are less than 1%, and there is substantial cancellation between the second-order Coulomb contribution and the full Breit contribution. The all-order calculations are in better agreement with experiment than the third-order calculations, as is to be expected. The overall agreement with experiment is seen to be excellent, except for the  $3d$  interval in P V.

In Table V, we give some comparisons of our results for the  $3p_{3/2}-3p_{1/2}$  and  $3d_{5/2}-3d_{3/2}$  fine-structure intervals with theoretical results from Refs. [24] and [25]. The value from Ref. [24] for the  $3p$  fine-structure interval in Na I was obtained using nonrelativistic MBPT including the polarization correction only. Omitted correlation corrections in Refs. [24]

TABLE V. Comparison of the present calculations of the fine-structure intervals ( $\text{cm}^{-1}$ ) of  $3p$  and  $3d$  states with other theoretical data.

Z		Present	Other	Other	Expt.
11	$3p_{3/2}-3p_{1/2}$	17.15	15.465 <sup>a</sup>		17.20
11	$3d_{5/2}-3d_{3/2}$	-0.048	-0.0449 <sup>b</sup>	-0.0428 <sup>c</sup>	-0.050
14	$3d_{5/2}-3d_{3/2}$	-1.06	-3.32 <sup>b</sup>	-1.64 <sup>c</sup>	-1.19

<sup>a</sup>NR MBPT [24].

<sup>b</sup>NR MBPT [25].

<sup>c</sup>Rel. HF [25].

TABLE VI. Comparison of reduced dipole matrix elements (a.u.) in length and velocity forms for Na.

Transition	Length	Velocity
$3p_{1/2}-3s_{1/2}$	3.531	3.531
$3p_{3/2}-3s_{1/2}$	4.994	4.991
$4s_{1/2}-3p_{1/2}$	3.576	3.574
$4s_{1/2}-3p_{3/2}$	5.068	5.067
$3d_{3/2}-3p_{1/2}$	6.802	6.806
$3d_{3/2}-3p_{3/2}$	3.046	3.047
$3d_{5/2}-3p_{3/2}$	9.137	9.143

and [25] explain the differences with the present work and with experiment. The results in Ref. [24] for the  $3d$  interval were obtained by two different methods: nonrelativistic MBPT including core polarization to first order in the spin-orbit coupling and to all orders in the Coulomb interaction (designated by superscript  $b$  in Table V), and a relativistic central-field approach using the Pauli approximation (designated by  $c$  in Table V). The differences between  $b$  and our data are due to relativistic effects and omitted correlation corrections. The agreement with  $c$  is unexpectedly good, owing to a fortuitous cancellation between second-order Coulomb correlation corrections and Breit corrections.

#### IV. REDUCED DIPOLE MATRIX ELEMENTS AND HYPERFINE CONSTANTS

##### A. $E1$ transitions

The SD wave functions are used to evaluate  $E1$  reduced matrix elements for  $3p_{1/2}-3s$ ,  $3p_{3/2}-3s$ ,  $4s-3p_{1/2}$ ,  $4s-3p_{3/2}$ ,  $3d_{3/2}-3p_{1/2}$ ,  $3d_{3/2}-3p_{3/2}$ , and  $3d_{5/2}-3p_{3/2}$  transitions in sodium and sodiumlike ions with  $Z=12-16$ . To evaluate these matrix elements, we followed the method outlined in Sec. II C. Single- and double-excitation amplitudes obtained from Eqs. (2), (3), and (5)–(7) were used to calculate the twenty terms in  $Z_{\text{val}}$ . Since the excitation amplitudes  $\rho_{mnab}$ , etc. occurring in the expressions for  $Z_{\text{val}}$  included partial waves with  $l \leq 6$ , the sums over excited states in  $Z_{\text{val}}$  were also limited to partial waves with  $l \leq 6$ . To estimate the truncation error caused by limiting the number of partial waves, we redid all calculations using  $l \leq 5$ , and found that resulting matrix elements were unchanged to four digits.

The level of agreement between length and velocity forms for electric-dipole transition matrix elements serves to measure the consistency of the theoretical formalism as well as

TABLE VII. Reduced dipole matrix elements (a.u.) in length form for sodiumlike ions.

Transition	Na I	Mg II	Al III	Si IV	P V	S VI
$3p_{1/2}-3s_{1/2}$	3.531	2.369	1.845	1.523	1.314	1.154
$3p_{3/2}-3s_{1/2}$	4.994	3.351	2.611	2.165	1.859	1.634
$4s_{1/2}-3p_{1/2}$	3.576	1.693	1.092	0.7959	0.6209	0.5058
$4s_{1/2}-3p_{3/2}$	5.068	2.404	1.552	1.133	0.8855	0.7226
$3d_{3/2}-3p_{1/2}$	6.802	4.158	3.074	2.436	2.013	1.712
$3d_{3/2}-3p_{3/2}$	3.046	1.862	1.376	1.091	0.9013	0.7667
$3d_{5/2}-3p_{3/2}$	9.137	5.587	4.130	3.273	2.705	2.301

TABLE VIII. Comparison of line strengths  $S$  (a.u.) for the  $3p$ - $3s$  transition in sodium with other theoretical and experimental data.

Method		$S$ ( $3p$ - $3s$ )
Present	SD <sup>a</sup>	37.39(1)
	Theory	
	SD [2]	37.51(2)
	SD [10]	37.38(11)
	MBPT [10]	37.65
	CCSD <sup>b</sup> [11]	37.56
	CI [12]	37.35
	CI <sup>b</sup> [12]	37.26
Expt.	$C_3$ analysis [26]	37.31(4)
	Beam-gas-laser spectroscopy [9]	37.26(5)
	Linewidth [27]	37.30(8)
	$C_3$ analysis [28]	37.33(12)

<sup>a</sup>Error estimate is based on difference of length and velocity forms.

<sup>b</sup>Corrected for relativistic effects using the ratio between DHF and HF values.

the accuracy of the numerical algorithms. A sample comparison of length and velocity forms for  $E1$  transitions in Na, where the correlation contribution is most important, is given in Table VI. The length and velocity forms are seen to agree to better than 0.05% for the seven transitions considered. The length-velocity agreement improves with increasing nuclear charge  $Z$  along the isoelectronic sequence.

In Table VII, we list length-form reduced dipole matrix elements for ions with  $Z = 11$ –16 for each of the seven transitions listed above. We estimate that the theoretical uncertainty is less than 0.05% for the data presented in this table.

New precise measurements recently became available for the  $3p$ - $3s$  transition in neutral sodium [9,26–28]. For a review of the recent experimental results, we refer the reader to the paper by Volz and Schmoranzner [9]. Comparisons of our results with the accurate *ab initio* calculations of  $3p$ - $3s$  line strengths in sodium from Refs. [2,10–12], and with the recent experimental line strengths from Refs. [9,26–28] are given in Table VIII. These comparisons are based on line strengths to amplify discrepancies and to facilitate comparisons with nonrelativistic calculations. (The  $3p$ - $3s$  line strength from the present relativistic calculation is the sum of the squares of the  $3p_{1/2}$ - $3s$  and  $3p_{3/2}$ - $3s$  reduced matrix elements.) The SD values from Refs. [2,10] were obtained from an all-order relativistic many-body calculation similar to the present one. In Ref. [11], an accurate nonrelativistic calculation of the  $3p$ - $3s$  matrix element was obtained using

TABLE X. Comparison of lifetimes (ns) of  $4s_{1/2}$  and  $3d_{3/2}$  levels in sodiumlike ions with available experimental data.

Z	$4s_{1/2}$			$3d_{3/2}$		
	Present	Expt.	Ref.	Present	Expt.	Ref.
Mg II	2.88	2.45(30) <sup>a</sup>	[34]	2.07	1.9(2)	[29]
Al III				0.721	0.905(30) <sup>a</sup>	[32]
Si IV	0.281	0.31(4)	[30]	0.392	0.42(5)	[30]
P V	0.136			0.263	0.32(2) <sup>b</sup>	[33]
S VI	0.0754	0.086(15)	[31]	0.198	0.20(1)	[31]

<sup>a</sup>The value is obtained by averaging over two decay branches. The experimental error quoted is due to a single branch.

<sup>b</sup>The lifetime of the  $3d^2D$  level.

the CCSD approach; this nonrelativistic matrix element was corrected for relativistic effects using a scaling factor determined by comparing relativistic and nonrelativistic Hartree-Fock matrix elements. Accurate nonrelativistic configuration-interaction (CI) calculations of the  $3s$ - $3p$  line strengths were performed in Ref. [12], and corrected for relativistic effects as explained above. Line strengths from the present calculation are in fair agreement with these other theoretical calculations. Moreover, our calculated line strength agrees with the most precise experimental value to better than 0.2%. The corresponding difference for the dipole matrix element is about 0.1%, which is smaller than the difference between theory and experiment for the  $3s$  hyperfine constant  $A$  in sodium, discussed below. It is worth noting that the accuracy could possibly be improved by including a set of triple excitations, since the CI calculations [12] of line strengths for Na I, which include a limited set of triples, give results closer to the most precise experimental value [26]. Comparing the scaled relativistic and nonrelativistic results from Ref. [12], one finds that relativistic corrections are about twice as large as the error estimate in the most precise experiment [26]. Thus, at this level of agreement between theoretical and experimental data, relativistic and higher-order correlation corrections are approximately the same size, emphasizing the importance of an *ab initio* relativistic approach.

Comparisons of our results with available experimental data Refs. [9,26,29–31] for  $3p_{1/2}$ - $3s_{1/2}$ ,  $3p_{3/2}$ - $3s_{1/2}$ , and  $3d_{5/2}$ - $3p_{3/2}$  transitions in sodiumlike ions are given in Table IX, where we list reduced matrix elements to eliminate the strong dependence of decay rates on photon energy. Our calculations agree with experimental values to within the experimental error bars for all three transitions in Mg II, Si IV,

TABLE IX. Comparison of reduced dipole matrix elements (a.u.) for sodiumlike ions with available experimental data.

Ion	$3p_{1/2}$ - $3s_{1/2}$			$3p_{3/2}$ - $3s_{1/2}$			$3d_{5/2}$ - $3p_{3/2}$		
	Present	Expt.	Ref.	Present	Expt.	Ref.	Present	Expt.	Ref.
Na I	3.531	3.5267(17)	[26]	4.994	4.9875(25)	[26]			
		3.5246(23)	[9]		4.9838(34)	[9]			
Mg II	2.369	2.376(9)	[29]	3.351	3.366(16)	[29]			
Si IV	1.523	1.53(3)	[30]	2.165	2.17(5)	[30]	3.273	3.1(2)	[30]
S VI	1.154	1.19(2)	[31]	1.634	1.64(3)	[31]	2.301	2.2(1)	[31]

TABLE XI. Magnetic dipole hyperfine constants  $A$  (MHz) for  $^{23}\text{Na}$ .

	$3s_{1/2}$	$3p_{1/2}$	$3p_{3/2}$	$4s_{1/2}$	$3d_{3/2}$	$3d_{5/2}$
DHF	623.5	63.39	12.59	150.7	0.5883	0.2522
SD	888.1	94.99	18.84	204.8	0.5314	0.1137
SD <sup>a</sup>	884.5(1.0)	92.4(2)	19.3(1)	202.2(3)		
CI <sup>b</sup>	882.2	94.04	18.80			
CCSD <sup>c</sup>	883.8	93.02	18.318			
MBPT <sup>d</sup>	860.9	91.40	19.80			
Expt.	885.81 <sup>e</sup>	94.42(19) <sup>f</sup> 94.44(13) <sup>j</sup>	18.79(12) <sup>g</sup> 18.534(15) <sup>k</sup>	202(3) <sup>h</sup>	0.527(25) <sup>i</sup>	0.1085(24) <sup>i</sup>

<sup>a</sup>Reference [2].<sup>b</sup>Reference [12].<sup>c</sup>Reference [11].<sup>d</sup>Reference [7].<sup>e</sup>Reference [36].<sup>f</sup>Reference [37].<sup>g</sup>Reference [39].<sup>h</sup>Reference [41].<sup>i</sup>Reference [42].<sup>j</sup>Reference [38].<sup>k</sup>Reference [40].

and S VI, except for the  $3p_{1/2}$ - $3s_{1/2}$  transition in S VI. For Na I, where high-precision experiment data are available, our data differ from experiment by about 0.1%.

In Table X, we compare our theoretical lifetimes for two-branch transitions, where the energy cannot be factored, with experimental values from Refs. [29–34]. The theoretical and experimental lifetimes agree to within the experimental error bars, except for 20% differences found for the  $3d_{3/2}$  states of Al III and P V. We attribute these differences to experimental errors, since the accuracy of the SD calculation is expected to improve with increasing nuclear charge along the isoelectronic sequence.

### B. Hyperfine constants $A$ and $B$

Calculations of hyperfine constants follow the same pattern as the calculations of reduced dipole matrix elements described in Sec. IV A. The magnetic moments and nuclear spins used in the present calculations are taken from Ref. [35]. In Table XI, we give the present SD values of the magnetic-dipole hyperfine constants  $A$  for  $^{23}\text{Na}$ , and compare our values with available theoretical [2,7,11,12] and experimental [36–42] data. The present SD value for  $A_{3s}$  disagrees with the very precise experimental value from Ref. [36] by about 0.25%. The agreement with other experimental values is at the level of 0.5%, except for  $A_{3d_{5/2}}$ . For this case the disagreement is 5%, and theoretical and experimental values differ by two standard deviations. The reason for this

TABLE XII. Magnetic dipole hyperfine constants  $A$  (MHz) for sodiumlike ions.

State	$^{25}\text{Mg}$ II	$^{27}\text{Al}$ III	$^{29}\text{Si}$ IV	$^{31}\text{P}$ V	$^{33}\text{S}$ VI
$3s_{1/2}$	−597.6	4885	−6060	18407	4910
$3p_{1/2}$	−103.4	1013	−1388	4488	1250
$3p_{3/2}$	−19.29	182.4	−245.2	783.4	216.8
$4s_{1/2}$	−163.4	1462	−1919	6070	1667
$3d_{3/2}$	−1.140	19.75	−39.65	165.4	55.02
$3d_{5/2}$	0.1196	−2.757	3.238	−2.520	2.358

relatively large disagreement is difficult to judge, since there are no other theoretical or experimental values for  $3d$  states in sodium.

The magnetic-dipole hyperfine constants  $A$  of the six states considered in sodiumlike ions are presented in Table XII. The precise experimental value for the  $3s$  state in sodiumlike  $^{25}\text{Mg}$ , given in Ref. [43],  $A(3s) = -596.254$  MHz, differs by 0.2% with the value  $-597.56$  MHz from the present work.

Values of electric quadrupole hyperfine constants  $B$  for  $3p_{3/2}$ ,  $3d_{3/2}$ , and  $3d_{5/2}$  states in  $^{23}\text{Na}$  can be found in Table XIII, where we list ratios of  $B$  to the nuclear quadrupole moment  $Q$ . The present SD calculation gives a higher value of ratio  $B/Q$  for the  $3p_{3/2}$  state of  $^{23}\text{Na}$  than found in previous accurate atomic calculations [11,12]. A possible reason is that our calculations are *ab initio* relativistic calculations, in contrast to the previous calculations of the  $B/Q$  ratio. The electric quadrupole interaction contains a factor  $1/r^3$ , which amplifies the behavior of wave functions near the nucleus. The motion of an electron in that region is relativistic, and the consequent increase of electron densities at small  $r$  leads to larger values of  $B/Q$  compared to nonrelativistic calculations. The  $s_{1/2}$  and  $p_{1/2}$  states are those most affected; thus the correlation contribution is modified by relativity more than the  $3p_{3/2}$  DHF contribution. For  $B_{3p_{3/2}}$ , the correlation

TABLE XIII. Quadrupole hyperfine coupling constants  $-B/Q$  (MHz/b) for  $^{23}\text{Na}$ .

	$3p_{3/2}$	$3d_{3/2}$	$3d_{5/2}$
DHF	15.76	0.2458	0.3502
SD	26.85	1.238	1.768
CI <sup>a</sup>	25.79		
CCSD <sup>b</sup>	26.14		

<sup>a</sup>Reference [12] with included relativistic correction using the ratio of DHF and HF values.

<sup>b</sup>Reference [11]. Relativistic correction was estimated by using factor from Ref. [44].

TABLE XIV. Contributions to the expectation value of the Breit operator (a.u.) for the  $3s_{1/2}$  state of Na.  $a[-b]=a \times 10^{-b}$ .

$B^{\text{DHF}}$	2.63[−5]
$B^{(1)}$	−1.83[−5]
$B^{(2)}$	−2.37[−6]
$B^{\text{SD}}$	5.60[−6]

contribution is about 40% of the total value. It follows that a scaling procedure based on the DHF value alone [44], such as used in nonrelativistic calculations [11,12], would underestimate the size of the relativistic corrections.

Combined with the experimental value  $B=2.724(30)$  MHz from Ref. [40], we obtain for  $^{23}\text{Na}$  a nuclear quadrupole moment  $Q=101.4(11)$  mb. The error in the value of  $Q$  is experimental. The theoretical error is 1% or less, based on the comparisons between theoretical and experimental values for removal energies, dipole matrix elements, and magnetic dipole hyperfine constants  $A$ . The “atomic” value of nuclear quadrupole moment obtained in this way is in agreement with the value  $Q=100.6(20)$  mb obtained in muonic experiments [45], and resolves the long-standing disagreement [12,46] between “atomic” and “muonic” values of the nuclear quadrupole moment of  $^{23}\text{Na}$ . The values of the  $B/Q$  for  $3d$  states given in Table XIII may aid in the experimental determination of  $A$  for these states.

### C. Breit corrections in the SD approximation

We give a breakdown of various contributions to the expectation value of the Breit operator for the  $3s_{1/2}$  state of Na

TABLE XV. Expectation values of the Breit operator for sodiumlike ions.

	$3s_{1/2}$	$3p_{1/2}$	$3p_{3/2}$	$4s_{1/2}$	$3d_{3/2}$	$3d_{5/2}$
Na I						
DHF	2.63[−5]	1.27[−5]	8.79[−6]	6.33[−6]	0.59[−7]	0.34[−7]
MBPT	1.14[−5]	0.87[−5]	2.84[−6]	2.53[−6]	−2.30[−8]	−2.60[−8]
SD	0.56[−5]	0.65[−5]	0.58[−6]	1.55[−6]	−2.69[−7]	−2.73[−7]
Mg II						
DHF	8.43[−5]	6.91[−5]	4.77[−5]	2.35[−5]	2.08[−6]	1.16[−6]
MBPT	4.06[−5]	4.64[−5]	1.80[−5]	1.09[−5]	−0.29[−6]	−0.93[−6]
SD	3.16[−5]	4.05[−5]	1.22[−5]	0.91[−5]	−2.04[−6]	−2.65[−6]
Al III						
DHF	1.70[−4]	1.72[−4]	1.18[−4]	5.15[−5]	1.29[−5]	7.09[−6]
MBPT	0.90[−4]	1.17[−4]	0.51[−4]	2.66[−5]	0.05[−5]	−4.13[−6]
SD	0.79[−4]	1.09[−4]	0.42[−4]	2.42[−5]	−0.36[−5]	−8.39[−6]
Si IV						
DHF	2.87[−4]	3.24[−4]	2.23[−4]	9.13[−5]	4.12[−5]	2.25[−5]
MBPT	1.64[−4]	2.27[−4]	1.07[−4]	5.11[−5]	0.70[−5]	−0.91[−5]
SD	1.51[−4]	2.15[−4]	0.96[−4]	4.82[−5]	0.03[−5]	−1.60[−5]
P V						
DHF	4.38[−4]	5.32[−4]	3.67[−4]	1.44[−4]	9.36[−5]	5.09[−5]
MBPT	2.65[−4]	3.82[−4]	1.90[−4]	0.86[−4]	2.45[−5]	−1.35[−5]
SD	2.51[−4]	3.68[−4]	1.78[−4]	0.83[−4]	1.59[−5]	−2.24[−5]
S VI						
DHF	6.27[−4]	8.01[−4]	5.52[−4]	2.12[−4]	1.75[−4]	9.53[−5]
MBPT	3.99[−4]	5.89[−4]	3.06[−4]	1.33[−4]	0.59[−4]	−1.41[−5]
SD	3.83[−4]	5.74[−4]	2.93[−4]	1.29[−4]	0.49[−4]	−2.44[−5]

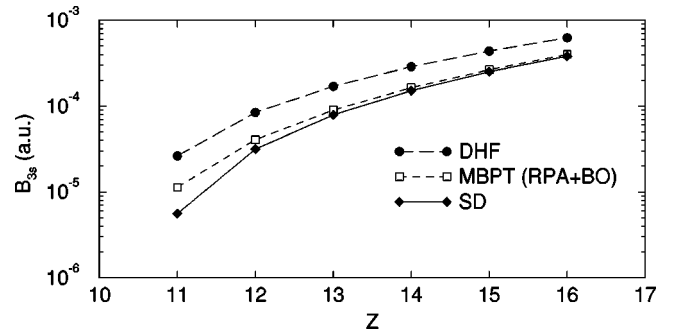


FIG. 6. Comparison of energy contributions due to Breit interaction for  $3s_{1/2}$  states along the sodium isoelectronic sequence. The DHF values are the first-order Dirac-Hartree-Fock contributions. The MBPT values are determined using the method given in Ref. [4]. The SD values are results of present work.

in Table XIV. The Breit correction, as discussed in Ref. [4], is significantly reduced by correlation contributions. The Dirac-Hartree-Fock value  $B^{\text{DHF}}=2.63 \times 10^{-5}$  a.u. is reduced to  $0.797 \times 10^{-5}$  a.u. by the one-body correlations  $B^{(1)}$ , and further to  $0.56 \times 10^{-5}$  a.u. by the two-body correlations  $B^{(2)}$ . Moreover, the resulting SD value is about two times smaller than that given by third-order MBPT,  $1.15 \times 10^{-5}$  a.u. Thus, higher-order diagrams contribute substantially to the Breit correction. To illustrate this point further, we plot DHF, MBPT, and SD calculations of the  $3s$  Breit energy shift along the isoelectronic sequence in Fig. 6. It can be seen that the MBPT and SD results approach each other as the ionic charge increases. Values of the Breit energy shift calculated in the DHF, MBPT, and SD approximations are given for the six states studied here in the range  $Z=11-16$  in Table XV.

## V. SUMMARY

The relativistic SD method including  $E_{v \text{ extra}}^{(3)}$  gives removal energies of  $3s$ ,  $3p$ ,  $3d$ , and  $4s$  states in Na I accurate to better than  $2 \text{ cm}^{-1}$  and, for ions with  $Z=12-16$ , gives energies that agree with experiment at the level  $1-20 \text{ cm}^{-1}$ , assuming Lamb-shift corrections are included for  $3s$  states. We find that  $E_{v \text{ extra}}^{(3)}$  increases with  $Z$  for  $Z < 20$ , and accounts for a substantial fraction of the correlation energy in this range. It is about 85% of the total third-order energy for  $Z=20-35$ . The fourth- and higher-order correlation corrections decrease with  $Z$  beyond  $Z=15$ , and become negligible (less the 1% of the correlation energy) for  $Z=20$ . Therefore, for  $Z > 20$ , accurate third-order calculations are sufficient to obtain high-precision results. The Breit correction is determined by evaluating the expectation value of the Breit operator using SD wave functions. Such a consistent calculation is important, considering the relatively large size of correlation corrections for this operator.

Magnetic-dipole hyperfine structure constants  $A$ , electric-quadrupole hyperfine constants  $B$ , and  $E1$  matrix elements were evaluated using SD wave functions for sodiumlike ions with  $Z=11-16$ . For each ion considered,  $A$  hyperfine constants were evaluated for  $3s$ ,  $3p_{1/2}$ ,  $3p_{3/2}$ ,  $4s$ ,  $3d_{3/2}$ , and  $3d_{5/2}$  states, and electric-dipole matrix elements were evaluated for the seven possible  $E1$  transitions between these states. Furthermore,  $B$  hyperfine constants were determined for the  $3p_{3/2}$ ,  $3d_{3/2}$ , and  $3d_{5/2}$  states of neutral sodium. Our comparison of  $E1$  transition amplitudes and hyperfine constants with available experimental data suggests that an accuracy of better than 0.3% was obtained for all of these matrix elements. We infer from our calculations of the  $B$  coefficient of Na that the value of electric-quadrupole moment of the  $^{23}\text{Na}$  nucleus is 101.4(11) mb, somewhat higher than all previous atomic calculations, and in good agreement with the value of 100.6(20) mb obtained in muonic atom measurements. To improve the accuracy of the present calculations of energies and matrix elements, it will be necessary to include triple excitations in the SD equations.

## ACKNOWLEDGMENTS

This work was supported in part by NSF Grant No. PHY95-13179. The authors owe debts of gratitude to Zu-Wei Liu for his help in developing the present SD codes, to L.J. Curtis and U. Volz for helpful discussions on transition lifetimes, and to P. Indelicato for sending values for the  $3s$  Lamb shift. U.I. Safronova also deserves thanks for useful advice on the manuscript.

## APPENDIX

We used two methods to extrapolate the partial-wave sequences for  $\delta E_v$ . In the first, we extrapolated all-order re-

TABLE XVI. Extrapolation of the partial-wave sequence for the  $3p_{1/2}$  state of Al III.

$l$	$\delta E_{3p_{1/2}}$	$E_{3p_{1/2}}^{(2)}$	Diff.
0	0.000430	0.000472	-0.000041
1	-0.000769	-0.000587	-0.000182
2	-0.008137	-0.007445	-0.000692
3	-0.009181	-0.008506	-0.000674
4	-0.009479	-0.008834	-0.000644
5	-0.009570	-0.008947	-0.000623
6	-0.009607	-0.008995	-0.000611
(4-5-6)	-0.009657		-0.000594
Total	-0.009657		-0.000661

sults using the scheme described in Ref. [1]. Briefly, we fit the partial-wave contributions  $\delta_l = \delta E_v(l) - \delta E_v(l-1)$  to a polynomial,

$$\delta_l = \frac{a_1}{l^4} + \frac{a_2}{l^5} + \frac{a_3}{l^6}, \quad (\text{A1})$$

and found the remainder of the sequence by summing  $\delta_l$  over the range  $l=7$  to  $\infty$  using the fit in Eq. (A1). In the second method, we made use of the fact that the second-order terms dominate the energy. We subtracted the second-order contributions  $E_v^{(2)}(l)$  [calculated with the basis set used to evaluate  $\delta E_v(l)$ ] from the all-order result  $\delta E_v(l)$ , and extrapolated the differences using Eq. (A1). This extrapolated tail was then added to a precise second-order energy calculated separately using a much larger basis set.

In Table XVI, we illustrate these two methods for the case of the  $3p_{1/2}$  state in Al III ( $Z=13$ ), where the precise second-order energy is  $E_{3p_{1/2}}^{(2)} = -0.009\,067$  a.u. In the first column, we list the number of partial waves included in the calculation; in the second column, we give the partial wave sequence for  $\delta E_{3p_{1/2}}$ ; in the third, we give the partial-wave sequence for  $E_{3p_{1/2}}^{(2)}$ ; and in the final column, we list the differences between the data in the second and third columns. In the row labeled (4-5-6), we give the extrapolated limit of the previous rows using the three-parameter fit to the values in rows  $l=4, 5$ , and 6. The value given at the bottom of the second column was found by direct extrapolation of  $\delta E_{3p_{1/2}}$ . The value listed at the bottom of the final column was found by extrapolating the differences and adding the precise second-order energy,  $-0.009\,067$  a.u. We define our uncertainty to be the difference between the results of these two extrapolation schemes; in this case we find  $E^{\text{corr}} = -0.009\,661(4)$  a.u. The uncertainty in this case is about  $1 \text{ cm}^{-1}$ . It should be emphasized that this is the numerical uncertainty only, and does not reflect missing physical effects.

- [1] S. A. Blundell, W. R. Johnson, Z. W. Liu, and J. Sapirstein, Phys. Rev. A **40**, 2233 (1989).  
 [2] Z. W. Liu, Ph.D. thesis, Notre Dame University, 1989.  
 [3] S. A. Blundell, W. R. Johnson, and J. Sapirstein, Phys. Rev. A **43**, 3407 (1991).

- [4] W. R. Johnson, S. A. Blundell, and J. Sapirstein, Phys. Rev. A **38**, 2699 (1988).  
 [5] K. T. Cheng, W. R. Johnson, and J. Sapirstein, Phys. Rev. Lett. **66**, 2960 (1991).  
 [6] I. Lindgren and J. Morrison, *Atomic Many-Body Theory*, 2nd

- ed. (Springer, Berlin, 1986), Chap. 15.
- [7] W. R. Johnson, M. Idrees, and J. Sapirstein, *Phys. Rev. A* **35**, 3218 (1987).
- [8] W. R. Johnson, Z. W. Liu, and J. Sapirstein, *At. Data Nucl. Data Tables* **64**, 279 (1996).
- [9] U. Volz and H. Schmoranzler, *Phys. Scr.* **T65**, 48 (1996).
- [10] C. Guet S. A. Blundell, and W. R. Johnson, *Phys. Lett. A* **143**, 384 (1990).
- [11] S. Salomonson and A. Ynnerman, *Phys. Rev. A* **43**, 88 (1991).
- [12] Per Jönsson, Anders Ynnerman, Charlotte Froese Fischer, Michel R. Godefroid, and Jeppe Olsen, *Phys. Rev. A* **53**, 4021 (1996).
- [13] G. E. Brown and D. G. Ravenhall, *Proc. R. Soc. London, Ser. A* **208**, 552 (1951).
- [14] W. R. Johnson, S. A. Blundell, and J. Sapirstein, *Phys. Rev. A* **37**, 307 (1988).
- [15] S. A. Blundell, D. S. Guo, W. R. Johnson, and J. Sapirstein, *At. Data Nucl. Data Tables* **37**, 103 (1987).
- [16] K. T. Cheng and W. J. Childs, *Phys. Rev. A* **31**, 2775 (1985).
- [17] A. Derevianko, W. R. Johnson, and Stephan Fritzsche, *Phys. Rev. A* **57**, 2629 (1998).
- [18] J. R. Fuhr, W. C. Martin, A. Musgrove, J. Sugar, and W. L. Wiese, *NIST Atomic Spectroscopic Database*, Ver. 1.1 January 1996. NIST Physical Reference Data. Online. National Institute of Standards and Technology. Available <http://physics.nist.gov/PhysRefData/contents.html>
- [19] P. J. Mohr and Y.-K. Kim, *Phys. Rev. A* **45**, 2727 (1991).
- [20] I. P. Grant, B. J. McKinzie, P. H. Norrington, D. F. Mayers, and N. C. Pyper, *Comput. Phys. Commun.* **21**, 207 (1980); B. J. McKinzie, I. P. Grant, and P. H. Norrington, *ibid.* **21**, 233 (1980).
- [21] Y.-K. Kim, D. H. Baik, P. Indelicato, and J. P. Desclaux, *Phys. Rev. A* **44**, 148 (1991).
- [22] T. A. Welton, *Phys. Rev.* **74**, 1157 (1948).
- [23] Charlotte Froese Fischer, *Can. J. Phys.* **54**, 1465 (1976).
- [24] L. Holmgren, I. Lindgren, J. Morrison, and A.-M. Mårtensson, *Z. Phys. A* **206**, 179 (1976).
- [25] I. Lindgren and A.-M. Mårtensson, *Phys. Rev. A* **26**, 3249 (1982).
- [26] K. M. Jones, P. S. Julienne, P. D. Lett, W. D. Phillips, E. Tiesinga, and C. J. Williams, *Europhys. Lett.* **35**, 85 (1996).
- [27] C. W. Oates, K. R. Vogel, and J. L. Hall, *Phys. Rev. Lett.* **76**, 2866 (1996).
- [28] E. Tiemann, H. Knöckel, and H. Richling, *Z. Phys. D* **37**, 323 (1996).
- [29] W. Ansbacher, Y. Li, and E. H. Pinnington, *Phys. Lett. A* **139**, 165 (1989).
- [30] S. T. Maniak, E. Trabert, and L. J. Curtis, *Phys. Lett. A* **173**, 407 (1993).
- [31] J. O. Ekberg, L. Engström, S. Bashkin, B. Denne, S. Huldt, S. Johansson, C. Jupèn, U. Litzèn, A. Trigueiros, and I. Martinson, *Phys. Scr.* **29**, 226 (1984).
- [32] J. A. Kernahan, E. H. Pinnington, J. A. O'Neill, R. L. Brooks, and K. E. Donnelly, *Phys. Scr.* **19**, 267 (1979).
- [33] A. E. Livingston, J. A. Kernahan, D. J. G. Irwin, and E. H. Pinnington, *Phys. Scr.* **12**, 223 (1975).
- [34] L. Liljegy, A. Lindgård, S. Mannervik, E. Veje, and B. Jelenkovič, *Phys. Scr.* **21**, 805 (1980).
- [35] P. Raghavan, *At. Data Nucl. Data Tables* **42**, 189 (1989).
- [36] A. Beckman, K. D. Böklen, and D. Elke, *Z. Phys.* **270**, 173 (1974).
- [37] J. Carlsson, P. Jönsson, L. Sturesson, and C. Froese Fischer, *Phys. Scr.* **46**, 394 (1992).
- [38] W. A. Wijngaarden and J. Li, *Z. Phys. D* **32**, 67 (1994).
- [39] U. Volz, M. Majerus, H. Liebel, A. Schmitt, and H. Schmoranzler, *Phys. Rev. Lett.* **76**, 2862 (1996).
- [40] W. Yei, A. Sieradzan, and M. D. Havey, *Phys. Rev. A* **48**, 1909 (1993).
- [41] K. H. Liao, R. Gupta, and W. Happer, *Phys. Rev. A* **8**, 2792 (1973).
- [42] B. Burghardt, B. Hoffman, and G. Meisel, *Z. Phys. D* **8**, 109 (1988).
- [43] W. M. Itano and D. J. Wineland, *Phys. Rev. A* **24**, 1364 (1981).
- [44] A. Rosèn and I. Lindgren, *Phys. Scr.* **6**, 109 (1972).
- [45] B. Jeckelmann, W. Beer, I. Beltrami, F. W. N. de Boer, G. de Chambrier, P. F. A. Goudsmit, J. Kern, H. J. Leisi, W. Ruckstuhl, and A. Vacchi, *Nucl. Phys. A* **408**, 495 (1983).
- [46] D. Sundholm and J. Olsen, *Phys. Rev. Lett.* **68**, 927 (1992).